IEEE Access
Multidisciplinary | Rapid Review | Open Access Journal

Received March 30, 2020, accepted April 6, 2020, date of publication April 13, 2020, date of current version April 29, 2020.

Digital Object Identifier 10.1109/ACCESS.2020.2987348

Decentralized Multi-Subgroup Formation Control With Connectivity Preservation and Collision Avoidance

JOONWON CHOI[1], YEONGHO SONG[1], SEUNGHAN LIM[2], CHEOLHYEON KWON[1], (Member, IEEE), AND HYONDONG OH[1], (Senior Member, IEEE)

[1]Ulsan National Institute of Science and Technology (UNIST), Ulsan 44919, South Korea
[2]Agency for Defense Development (ADD), Daejeon 34186, South Korea

Corresponding author: Hyondong Oh (h.oh@unist.ac.kr)

This work was supported in part by the Study on the Flocking and Networking for Small UAV Groups funded by the Agency for Defense Development, in part by the Basic Science Research Program through the National Research Foundation of Korea (NRF) funded by the Ministry of Education under Grant 2017R1D1A1B03029992, and in part by the Development of Drone System for Ship and Marine Mission of Civil Military Technology Cooperation Center under Grant 18-CM-AS-22.

ABSTRACT This paper proposes a formation control algorithm to create separated multiple formations for an undirected networked multi-agent system while preserving the network connectivity and avoiding collision among agents. Through the modified multi-consensus technique, the proposed algorithm can simultaneously divide a group of multiple agents into any arbitrary number of desired formations in a decentralized manner. Furthermore, the agents assigned to each formation group can be easily reallocated to other formation groups without network topological constraints as long as the entire network is initially connected; an operator can freely partition agents even if there is no spanning tree within each subgroup. Besides, the system can avoid collision without loosing the connectivity even during the transient period of formation by applying the existing potential function based on the network connectivity estimation. If the estimation is correct, the potential function not only guarantees the connectivity maintenance but also allows some extra edges to be broken if the network remains connected. Numerical simulations are performed to verify the feasibility and performance of the proposed multi-subgroup formation control.

INDEX TERMS Collision avoidance, decentralized control, formation control, graph theory, multi-agent systems.

I. INTRODUCTION

With the remarkable progress of the Multi-Agent System (MAS) in recent years, there have been innovative applications within the MAS framework. In comparison with a single agent, the MAS can deal with complex missions that require the cooperative action among agents. For instance, multiple agents can jointly maximize the visibility of the target for better tracking performance [20], [25]. In [16], mobile robots were utilized as the supplementary Ultra Wide Band (UWB) nodes to enhance target localization accuracy in the 3-D environment. A cooperative searching strategy to identify contamination sources in hazardous areas was also proposed in [24] whereas novel velocity-aware motion planning algorithms with collision avoidance were proposed in [13], [14] for the decentralized MAS.

Forming a certain shape configuration is one of the most fundamental and widely-performed missions among various applications of the MAS. The MAS can achieve better efficiency in diverse circumstances by maintaining the designated formation configuration [21]. For instance, fuel consumption can be reduced by creating a tight V-shape formation among fixed-wing aerial vehicles [1], [2], [6]. Along with in-depth theoretical improvement of the MAS, there have been several real world experiments to implement formation control algorithms [27], [28].

Aforementioned approaches mainly focus on a single formation. Practical circumstances, however, may require several missions with different formations. In particular, to complete a multi-objective mission efficiently, the MAS

The associate editor coordinating the review of this manuscript and approving it for publication was Xiwang Dong.

This work is licensed under a Creative Commons Attribution 4.0 License. For more information, see https://creativecommons.org/licenses/by/4.0/

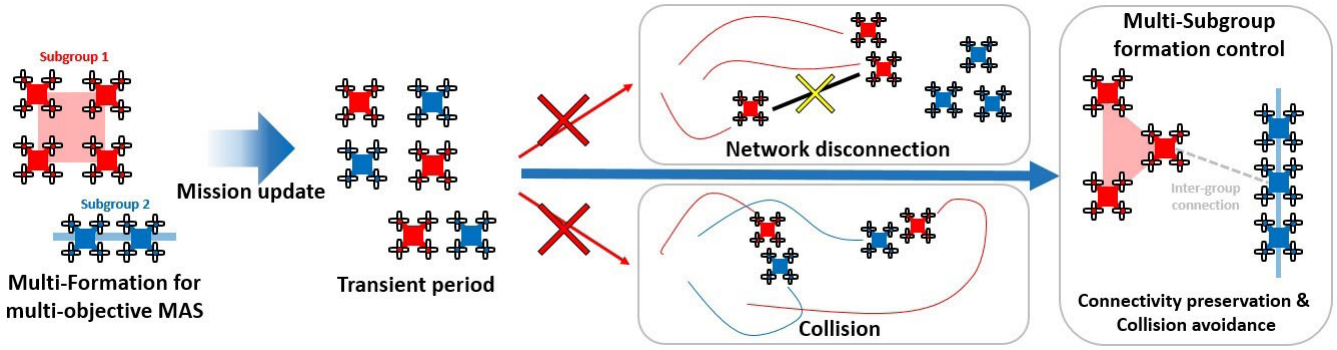

FIGURE 1. Concept of multiple subgroup formation.

might need to establish a multi-formation control algorithm. Nevertheless, there have been relatively few studies for creating multiple formations simultaneously [5], [9], [11], [17], [26]. In our preliminary research, the formation algorithm which divides the MAS into several V-shape formations was proposed [4]. However, due to complex interaction between different sub-formation groups during the transient phase, the convergence of the entire MAS may not be guaranteed; they are subject to initial position and velocity conditions. Motivated by this, we attempt to further improve the reliability and the flexibility of the multi-formation control in decentralized manner.

For the real world application, the multi-subgroup formation control should take account of collision avoidance and the connectivity maintenance while realizing the desired formations. This feature is particularly important for the heterogeneous MAS with multi-objective missions which require agents with different capabilities (e.g. sensing, agility, or operation time) and different desired formations as illustrated in Fig. 1. For instance, in [29], the task allocation algorithm motivated from the ant colony was introduced. In the paper, the algorithm allocates the tasks according to UAVs' capability for reconnaissance and destruction of the target. During the procedure, the allocated tasks can be varied due to unexpected enemy threat. However, if the connectivity within the MAS network is unreliable or the UAVs collide with each other, the MAS cannot accomplish the mission even with the proper task allocation.

In [7], [18], the authors introduced the hybrid potential function which can prevent the collision among MAS agents. At the same time, the potential function also inhibits the MAS from the disconnection via the decentralized network connectivity estimator, accomplishing a lattice formation in a decentralized manner. One of the benefits of the above approach is that it allows connection between agents to be broken if the entire network does not lose the spanning tree. Accordingly, unlike other connectivity preservation strategies which forbid existing edges to be broken, the designed potential function provides the MAS flexibility to perform formation missions. In this paper, we modify the existing potential function to adapt for general formation control. As a result, our proposed algorithm can ensure connectivity of the MAS even during the transient period of multi-formation without collision.

The network topology is also challenging part to achieve the multi-subgroup formation of the MAS. In [11], Han *et al*. proposed the leader-following protocol capable of generating multiple formations in the undirected network; however, agents in each formation need to be jointly connected. In other words, the restrictive network condition must be satisfied for the successful multi-formation control. It can impose a significant limitation on allocating agents since the entire MAS structure is constrained by the network condition. The similar limitation can be found in related studies [5], [9], [26]. For instance, in [17], the authors proposed the multi-formation control through the leader-following approach with the event-trigger strategy, but it also requires the spanning tree within subgroups. To address the above issues, the multi-consensus approach [10] can be applied as an alternative solution. In the multi-consensus, no subgroup network connectivity is required to reach different sets of final states. If the entire network is initially connected, the MAS achieves multiple consensuses.

In this paper, we propose a decentralized multi-subgroup formation control algorithm which can secure the network connectivity within the MAS at all times including the transient period of partition. The network condition considered in this work is modeled as an undirected time-varying graph that relies on the limited communication range. By modifying the multi-consensus algorithm from [10], the MAS can be distributed into multiple subgroup formations if the network is initially connected; the algorithm does not require any subgroup network condition as illustrated in Fig. 2. Their connectivity will be preserved without collision by the potential function approach based on [7], [18]. As a result, the proposed algorithm can flexibly change the formation shape and allocate agents to other formations regardless of network topology. The entire procedure is designed in a decentralized way. The proposed algorithm is theoretically proven to be stable in the sense of Lyapunov and numerically validated with illustrative simulation examples.

The rest of the paper is organized as follows. In Section II, basic preliminaries for the graph theory and multi-consensus are introduced. In Section III, a decentralized

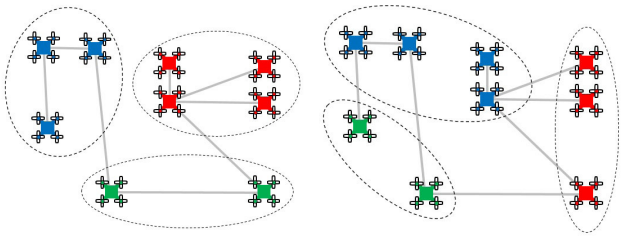

(a) Conventional methods (b) Multi-Consensus approach

FIGURE 2. Examples of grouping method for the MAS agents.

multi-subgroup formation control law is proposed with its stability proof. Numerical simulation results are provided in Section IV. Lastly, conclusions and future work are given in Section V.

II. PRELIMINARIES

A. GRAPH THEORY

Some basic concepts about algebraic graph theory are introduced here. Most notations are based on [19]. Let us define $\mathcal{G} = (\mathcal{V}, \mathcal{E})$ as the undirected graph with a vertex set $\mathcal{V} = \{1, 2, \ldots, n\}$ and an edge set $\mathcal{E} = \{e_{ij} \mid i, j \in \mathcal{V}, i \neq j\}$. n is the number of agents. An adjacency matrix which has (i, j) element as a_{ij} is represented as $\mathcal{A} \in \mathbb{R}^{n\times n}$. In the undirected graph, the agent j can obtain information of the agent i if there exists e_{ij} and vice versa. A set of neighbours of the agent i is defined as $\mathcal{N}_i = \{j \mid e_{ij} \in \mathcal{E}\}$. $a_{ij} = 1$ only when $e_{ij} \in \mathcal{E}$ and $a_{ij} = 0$ if not. $a_{ii} = 0 \ \forall i \in \mathcal{V}$ and a $n \times n$ degree matrix $\mathcal{D} := diag\{d_1, d_2, \ldots, d_n\}$ where $d_i = \sum_{j=1}^{n} a_{ij}$. The unweighted Laplacian matrix $\mathcal{L}$ can be expressed as

$$\mathcal{L} = \mathcal{D} - \mathcal{A}.$$

In the adjacent matrix, $\mathcal{A}$, its element can represent the communication strength between agents rather than just be a binary value. Consider the second-order multi-agent system with n agents whose dynamics can be described as

$$\begin{cases} \dot{x}_i(t) = v_i(t), \\ \dot{v}_i(t) = u_i(t), \quad \forall i \in \mathcal{V} \end{cases} \tag{1}$$

where $x_i(t) \in \mathbb{R}$ and $v_i(t) \in \mathbb{R}$ are the position and velocity of the agent i at time t, respectively. $u_i(t)$ is to be designed later. Although all states are assumed to be the one-dimensional throughout the paper, the same approach can be readily extended to multiple dimensions using the Kronecker product. The proximity-limited communication model with respect to the relative distance between agents i and j is

$$\bar{a}_{ij}(\|x_{ij}(t)\|) = \begin{cases} 1, & \|x_{ij}(t)\| \in [0, \tau R) \\ \frac{1}{2}[1 + \cos(\pi \frac{\frac{\|x_{ij}(t)\|}{R} - \tau}{1-\tau})], & \|x_{ij}(t)\| \in [\tau R, R) \\ 0, & \|x_{ij}(t)\| \in [R, \inf) \end{cases} \tag{2}$$

where τ is a communication decay rate, R is the maximum communication range, $x_{ij}(t) = x_i(t) - x_j(t)$, and $\|\cdot\|$ is the 2-norm. The model is borrowed from [7]. Then, similar to unweighted graph, $\overline{\mathcal{A}}$ can be defined as a $n \times n$ matrix whose (i, j) element is $\bar{a}_{ij}$, $\overline{\mathcal{D}} := diag\{\overline{d}_1, \overline{d}_2, \ldots, \overline{d}_n\}$, and $\overline{d}_i = \sum_{j=1}^{n} \bar{a}_{ij}$. The weighted Laplacian matrix is defined as

$$\overline{\mathcal{L}} = \overline{\mathcal{D}} - \overline{\mathcal{A}}. \tag{3}$$

We want to emphasize that each element of $\overline{\mathcal{L}}$ is continuous function with respect to the relative distance between the agents. Meanwhile, the elements of $\mathcal{L}$ are fixed at given $\mathcal{G}$ whereas they may jump as $\mathcal{G}$ varies with the time.

A path is defined as a finite sequence of edges in $\mathcal{G}$. If there exists a path from one node to all other nodes, i.e., every node is reachable from the others, the graph is connected. Furthermore, let $\lambda_1 \leq \lambda_2 \leq \cdots \leq \lambda_n$ be the eigenvalues of $\bar{\mathcal{L}}$ with corresponding unit eigenvectors $\nu_1, \ \nu_2, \ \cdots, \ \nu_n$. If the graph is connected, $\lambda_1 = 0$ and $\nu_1 = \frac{1}{\sqrt{n}} 1_n$. Also, $\lambda_2 > 0$ is called as the connectivity of the graph, which determines the convergence performance of the corresponding MAS. In this paper, notation 1_n is used for the n-column vector with all entries as 1 and 0_n as 0. Besides, unless otherwise stated, all graphs are considered to be the undirected graph and the connectivity is calculated from the weighted Laplacian matrix, $\overline{\mathcal{L}}$.

B. MULTI-CONSENSUS

In the second-order multi-agent system (1), the agents i and j are said to reach stationary consensus if they satisfy the following condition [10]:

$$\begin{cases} \lim_{t\to\infty} \|x_i(t) - x_j(t)\| = 0, \\ \lim_{t\to\infty} v_i(t) = \lim_{t\to\infty} v_j(t) = 0 \end{cases} \tag{4}$$

The consensus of agents implies that their states reach an agreement. By achieving identical states, the MAS can accomplish the collective behavior.

Lemma 1 (Multi-Consensus [10]): If there exists a directed spanning tree in the second-order multi-agent system with n agents, the system can reach multiple consensuses using $\widehat{\mathcal{L}}$, defined as

$$\widehat{\mathcal{L}} = \begin{bmatrix} \mathcal{L}_{11} & \frac{\omega_1}{\omega_2}\mathcal{L}_{12} & \cdots & \frac{\omega_1}{\omega_n}\mathcal{L}_{1n} \\ \frac{\omega_2}{\omega_1}\mathcal{L}_{21} & \mathcal{L}_{22} & \cdots & \frac{\omega_2}{\omega_n}\mathcal{L}_{2n} \\ \vdots & \vdots & \ddots & \vdots \\ \frac{\omega_n}{\omega_1}\mathcal{L}_{n1} & \frac{\omega_n}{\omega_2}\mathcal{L}_{n2} & \cdots & \mathcal{L}_{nn} \end{bmatrix}$$

where ω_i is the intelligence degree for the agent i and $\mathcal{L}_{ij}$ denotes the (i, j) element of the Laplacian matrix $\mathcal{L}$.

In the multi-consensus, agents with the identical intelligence degree achieve common consensus, i.e., the agents i and j satisfy (4) if $\omega_i = \omega_j$. Accordingly, the MAS can be separated arbitrary number of clusters by assigning the proper intelligence degrees. This is distinct characteristic of the multi-consensus in comparison with conventional consensus protocols that converge all agents to the same state. This feature allows the MAS to be clustered into multiple subgroup formations. More detailed explanations can be found in [10].

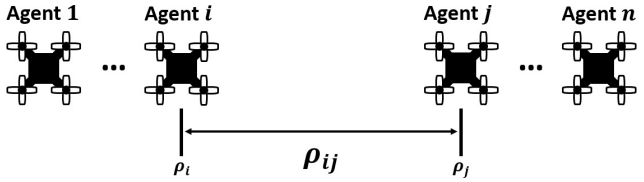

FIGURE 3. The definition of ρ_{ij} and corresponding formation.

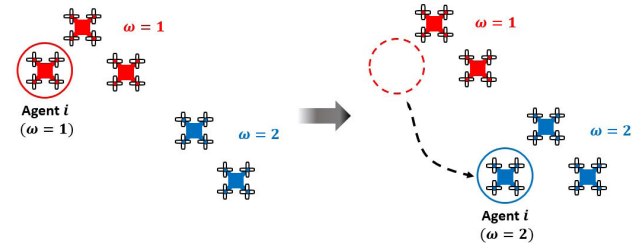

FIGURE 4. Simple formation reallocation via ω_i.

III. MAIN RESULT

This section proposes the multi-subgroup formation control and theoretically proves its stability using the Lyapunov function approach.

A. DECENTRALIZED MULTI-SUBGROUP FORMATION CONTROL

Consider the MAS with the dynamics described in (1). ρ_i is the reference state for the agent i which determines the formation shape. The required relative position for a desired formation is defined by the difference of the constants, $\rho_{ij} = \rho_i - \rho_j$, as shown in Fig. 3. Then, for each formation subgroup, the relative configurations between the members of the subgroup are imposed as

$$x_{ij} = \rho_{ij}, \quad \forall i, j \in \mathcal{V},\ i \neq j,\ \omega_i = \omega_j. \tag{5}$$

Note that time index t is omitted for the brevity. According to [21], this can be classified as the displacement-based formation. Unlike the distance-based formation which may flip or rotate the designated figure, this method determines the unique configuration for the MAS.

This approach can provide significant synergy with the aforementioned multi-consensus algorithm. By simply changing ω_i, $\forall i \in \mathcal{V}$, the allocation of agents into formations can be dynamically reconfigured. Not only the distance between subgroups, but also the subgroup each agent is assigned to is determined by ω_i [4]. After the individual agent receives their formation subgroup information that are specified by ω_i and ρ_i, the user does not have to manually designate any parameter. The system will autonomously reshape according to the desired condition as illustrated in Fig. 4. Moreover, the only network topological constraint is that the network needs to be initially connected, i.e., no connectivity within each subgroup is required.

It is worthwhile noting that although ρ_i and ω_i are assumed to be determined by an operator for the sake of simplicity in this paper, it can be readily determined by relevant task allocation algorithms [3], [29] and, if needed, depending on the mission requirement.

Definition 1 (Quasi-Formation): Traditionally, it is assumed that a formation is completed when (5) *is satisfied. However, similar to the concept of quasi-α-lattice in [22], we consider the formation within a certain error bound, $\delta > 0$. This yields*

$$\rho_{ij} - \delta \leq x_{ij} \leq \rho_{ij} + \delta, \quad \forall i, j \in \mathcal{V},\ i \neq j,\ \omega_i = \omega_j \tag{6}$$

when the formation is established. More specifically, the formation has a shape very close to the configuration represented by ρ_{ij}, but it has a certain error bounded by δ, given as

$$\delta = \max_{\omega_i = \omega_j} \|x_{ij} - \rho_{ij}\|$$

when the system is converged. In this paper, we define this kind of formation as quasi-formation.

By modifying the original multi-consensus control algorithm, the following multi-subgroup formation control law can be proposed:

$$u_i = -\sum_{j \in \mathcal{N}_i} \left[\alpha(\overline{x_i} - \frac{\omega_i}{\omega_j}\overline{x_j}) + \omega_i^2 \nabla_{x_i} V_{ij}^c \right] - \beta v_i \tag{7}$$

where $\overline{x}_k = x_k - \rho_k$, $k = 1, 2, \ldots, n$, and $\alpha, \beta > 0$. V_{ij}^c is the differentiable potential function modified from [7], given as

$$V_{ij}^c = \begin{cases} \| \frac{1}{\|x_{ij}\|} - \frac{1}{s} \|^{k_1} \frac{1}{(\lambda_{2,i} - \epsilon)^{k_2}}, & \|x_{ij}\| \in (0, s) \\ 0, & \|x_{ij}\| \in [s, R') \\ \frac{k_3}{2} \left[\frac{1 - cos(\pi \frac{\|x_{ij}\| - R'}{R - R'})}{(\lambda_{2,i} - \epsilon)^{k_2}} \right], & \|x_{ij}\| \in [R', R) \\ \frac{k_3}{(\lambda_{2,i} - \epsilon)^{k_2}}, & otherwise. \end{cases} \tag{8}$$

where $k_1 > 1$, $k_2 > 1$, and $k_3 > 0$. s is the repulsive range, R' is the formation-limit range, $\lambda_{2,i}$ is agent i's estimation of the connectivity (λ_2), and $\epsilon > 0$ is the connectivity lower bound.

V_{ij}^c is conditioned by the following three distinct regions with respect to the norm of the relative distance, $\|x_{ij}\|$.

1) $\|x_{ij}\| \in (0, s)$: In this bound, agents repel other agents whose relative distance is smaller than s. The less it is, the stronger the input is applied so that the MAS can achieve the collision avoidance.
2) $\|x_{ij}\| \in [s, R')$: This is the additionally added region in comparison with the potential function in [7]. The potential function in the region does not have any influence to both agent i and j. As a result, the agents can concentrate on the formation control task without the interference for the connectivity preservation and collision avoidance. Without this region, the uncertainty of the quasi-formation (δ) becomes significantly large when it converges. The stronger $\nabla_{x_i} V_{ij}^c$ applied on the system, the more the formation shapes are distorted. To

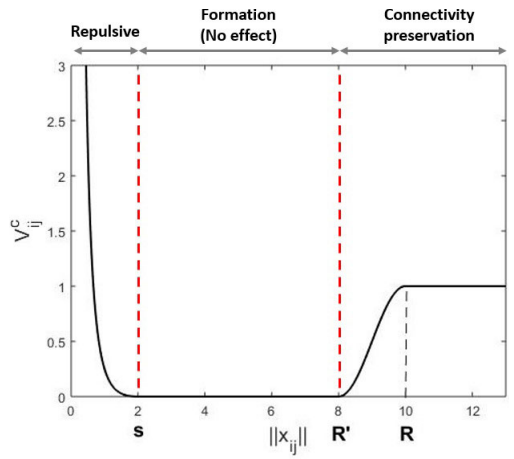

FIGURE 5. Graph of V_{ij}^c with the constant connectivity ($\lambda_{2,i}$) drawn for the illustration purpose.

avoid this situation, $[s, R')$ acts as an bounded space for the formation. It will be analytically discussed in Theorem 1 and its proof.

3) $\|x_{ij}\| \in [R', \infty)$: This region prevents the edges from disconnection. V_{ij}^c smoothly increases from R' and reaches a constant value at R. One may easily notice that V_{ij}^c does not reach infinite value in $[R', \infty)$ unless $\lambda_{2,i} \to \epsilon$, in contrast to $(0, s)$. This allows the edges to be broken if necessary. Accordingly, the network is flexible to perform the given missions. Nevertheless, as $\lim_{\lambda_{2,i}\to\epsilon} V_{ij}^c = \infty$ in (8), the estimated connectivity ($\lambda_{2,i}$) does not go below ϵ, which means the connectivity of the MAS is guaranteed.

Fig. 5 is the graph of V_{ij}^c using $k_1 = k_2 = 2, k_3 = 1, s = 2$, $R' = 8, R = 10, \lambda_{2,i} = 2$, and $\epsilon = 1$. As mentioned above, V_{ij}^c induces a large repulsive force as the relative distance becomes smaller than s. The potential function has no effect, i.e., 0 value in $[s, R')$, and maintains connectivity in $[R', \infty)$. If $\lambda_{2,i}$ gets closer to ϵ, not a constant value, the converged value of V_{ij}^c at $\|x_{ij}\| = R$ becomes larger and the network guarantees the connectivity all the time. It will be analytically proved in Theorem 1.

Due to the aforementioned characteristic in $[s, R')$, the desired formation configuration should be settled down on $[s, R')$. In other words, for two distinct agents i and j, the following inequality should be satisfied:

$$0 < s \leq \|\rho_{ij}\| \leq R', \quad \forall i, j \in \mathcal{V},\ \omega_i = \omega_j,\ i \neq j. \tag{9}$$

Otherwise, the potential function would distort the formations seriously. By satisfying (9), the MAS can generate quasi-formations with allowable δ.

To compute V_{ij}^c, the connectivity information (λ_2) is required. Although calculating the connectivity (λ_2) is a centralized task, an individual agent can estimate it ($\lambda_{2,i}$) in a distributed manner [30] through the PI average consensus estimator [8]. For the completeness of the paper, the PI average consensus estimator is briefly introduced, which can be represented as

$$\begin{aligned}\dot{z}^i &= \gamma(\zeta^i - z^i) - K_P \sum_{j\in\mathcal{N}_i}\left[z^i - z^j\right] + K_I \sum_{j\in\mathcal{N}_i}\left[\eta^i - \eta^j\right],\\ \dot{\eta}^i &= -K_I \sum_{j\in\mathcal{N}_i}\left[z^i - z^j\right],\end{aligned} \tag{10}$$

where K_P, K_I, and γ are positive constants. Let the agent i hold a certain scalar value $\zeta^i(t)$, $i = 1, 2, \ldots, n$ in the network with n agents. z^i is the estimation of $\frac{1}{n}\sum_{j=1}^n \zeta^j(t)$ for the agent i. In other words, z^i is the agent i's estimation of average of the $\zeta(t)$ values among the network. The entire network can share average information when the estimator converges. More details can be found in [8].

λ_2 can then be estimated by utilizing two PI average consensus estimators [30]. Let z_1^i be the agent i's estimation of $\frac{1}{n}\sum_{j=1}^n \bar{\nu}_j$, where $\bar{\nu} = [\bar{\nu}_1, \bar{\nu}_2, \ldots, \bar{\nu}_n]^T$ is the eigenvector corresponding to λ_2. $\bar{\nu}_j$ is the j-th element of $\bar{\nu}$. In the same way, define z_2^i as the estimation of $\frac{1}{n}\sum_{j=1}^n (\bar{\nu}_j)^2$. Then, the update law for $\bar{\nu}_i$ can be written as

$$\dot{\bar{\nu}}_i = -c_1 z_1^i - c_2 \sum_{j\in\mathcal{N}_i} \bar{a}_{ij}(\bar{\nu}_i - \bar{\nu}_j) - c_3(z_2^i - 1)\bar{\nu}_i \tag{11}$$

and the estimation of the connectivity from the agent i is obtained by

$$\lambda_{2,i} = \frac{c_3}{c_2}(1 - z_2^i) \tag{12}$$

where $c_2 > 0$ and $c_3,\ c_1 > n(n-1)c_2$. Through the above process, each agent can estimate the actual connectivity of the network(λ_2) in a distributed way, as long as the network is connected.

In this paper, it is assumed that the estimator converges to the steady state quickly and the error between the estimation and the actual connectivity is negligible, i.e., $\lambda_{2,i} \approx \lambda_2$, $\forall i \in \mathcal{V}$. Besides, note that λ_2 is obtained from $\bar{\mathcal{L}}$ in (3).

Definition 2: For the proposed input (7)*, a positive definite Lyapunov candidate function is defined as:*

$$V = \frac{1}{2}\sum_{i=1}^n \sum_{j\in\mathcal{N}_i}\left[V_{ij}^c + \alpha\hat{x}_i(\hat{x}_i - \hat{x}_j)\right] + \frac{1}{2}\sum_{i=1}^n \hat{v}_i^2 \tag{13}$$

where $\hat{x}_i$ *and* $\hat{v}_i$ *are* $\frac{\overline{x_i}}{\omega_i}$ *and* $\frac{v_i}{\omega_i}$*, respectively.*

To prove the stability of the system, two cases should be considered. One is when the network is static and the other is when it is dynamic. This is because $\lambda_{2,i}$ relies on the proximity communication model (2) which is continuous with respect to the relative distance between agents(x_{ij}), whereas V depends on $\mathcal{L}$, the piecewise continuous function as $\mathcal{G}$ varies with the time. This requires to analyze different Lyapunov functions per each graph for the stability proof. Accordingly, we first prove the stability when the network topology is fixed in Theorem 1 and extend the proof for the dynamic network.

Theorem 1: By using the proposed control law in (7), the MAS (1) with the static network can achieve any

number($\leq n$) of quasi-formations. In addition, the connectivity of the MAS never goes below ϵ and the collision is avoided, if the following conditions are satisfied:

1) $\omega_i \neq 0,\ \forall i \in \mathcal{V}$
2) $\lambda_{2,i}(0) > \epsilon,\ \forall i \in \mathcal{V}$
3) $|\mathrm{V}(0)| \ll \infty$, i.e., V(0) is bounded and
4) (9) is satisfied

Proof: To compute the derivative of V with respect to time, we first calculate $\dot{V}_{ij}^c$. Since $\dot{V}_{ij}^c$ is the function of x_i and x_j, using the chain rule,

$$\dot{V}_{ij}^c = v_i \nabla_{x_i} V_{ij}^c + v_j \nabla_{x_j} V_{ij}^c = \dot{V}_{ji}^c.$$

Since the network is undirected, if V_{ij}^c exists, V_{ji}^c also exists. Accordingly,

$$\frac{1}{2}\sum_{i=1}^{n}\sum_{j\in\mathcal{N}_i} \dot{V}_{ij}^c = \sum_{i=1}^{n}\sum_{j\in\mathcal{N}_i} v_i \nabla_{x_i} V_{ij}^c.$$

It is the same for $\alpha\hat{x}_i(\hat{x}_i - \hat{x}_j)$, yielding the following equation:

$$\frac{1}{2}\sum_{i=1}^{n}\sum_{j\in\mathcal{N}_i} \mathrm{d}[\alpha\hat{x}_i(\hat{x}_i - \hat{x}_j)]\mathrm{d}t = \sum_{i=1}^{n}\sum_{j\in\mathcal{N}_i} \alpha\hat{v}_i(\hat{x}_i - \hat{x}_j)$$

As a result, the derivative of V can be written as

$$\begin{aligned}\dot{\mathrm{V}} &= \frac{1}{2}\sum_{i=1}^{n}\sum_{j\in\mathcal{N}_i}[v_i\nabla_{x_i}V_{ij}^c + v_j\nabla_{x_j}V_{ij}^c + \alpha\hat{v}_i(\hat{x}_i - \hat{x}_j) \\ &\quad + \alpha\hat{x}_i(\hat{v}_i - \hat{v}_j)] + \sum_{i=1}^{n}\hat{v}_i\dot{\hat{v}}_i \\ &= \sum_{i=1}^{n}\sum_{j\in\mathcal{N}_i}\left[v_i\nabla_{x_i}V_{ij}^c + \alpha\hat{v}_i(\hat{x}_i - \hat{x}_j)\right] + \sum_{i=1}^{n}\hat{v}_i\dot{\hat{v}}_i.\end{aligned}$$

In the equation, the following holds

$$\sum_{i=1}^{n}\sum_{j\in\mathcal{N}_i}\alpha\hat{v}_i(\hat{x}_i - \hat{x}_j) = \alpha\hat{v}^T\mathcal{L}\hat{x}$$

$$\sum_{i=1}^{n}\hat{v}_i\dot{\hat{v}}_i = \sum_{i=1}^{n}\frac{\hat{v}_i u_i}{\omega_i} = \hat{v}^T\hat{u}$$

where $\hat{v} = [\hat{v}_1, \hat{v}_2, \ldots, \hat{v}_n]^T$, $\hat{x} = [\hat{x}_1, \hat{x}_2, \ldots, \hat{x}_n]^T$, and $\hat{u} = [\frac{u_1}{\omega_1}, \frac{u_2}{\omega_2}, \ldots, \frac{u_n}{\omega_n}]^T$. If we define

$$V^c = [\sum_{j\in\mathcal{N}_1}\nabla_{x_1}V_{1j}^c, \sum_{j\in\mathcal{N}_2}\nabla_{x_2}V_{2j}^c, \ldots, \sum_{j\in\mathcal{N}_n}\nabla_{x_n}V_{nj}^c]^T,$$

$\dot{\mathrm{V}}$ can be rewritten as

$$\begin{aligned}\dot{\mathrm{V}} &= \sum_{i=1}^{n}\sum_{j\in\mathcal{N}_i}(v_i\nabla_{x_i}V_{ij}^c) + \alpha\hat{v}^T\mathcal{L}\hat{x} + \hat{v}^T\hat{u} \\ &= v^T V^c + \alpha\hat{v}^T\mathcal{L}\hat{x} + \hat{v}^T\hat{u}.\end{aligned}$$

Here, $v = [v_1, v_2, \ldots, v_n]^T$. Now, let $\Lambda := diag[w_1, w_2, \ldots, w_n]$ and $u = [u_1, u_2, \ldots, u_n]^T$. One can easily notice $\hat{v} = \Lambda^{-1}v$, $\hat{x} = \Lambda^{-1}\bar{x}$, and $\widehat{\mathcal{L}} = \Lambda\mathcal{L}\Lambda^{-1}$ and from the fact that

$$\hat{u} = \Lambda^{-1}u = \Lambda^{-1}(-\alpha\widehat{\mathcal{L}}\bar{x} - \Lambda^2 V^c - \beta v), \tag{14}$$

the time derivative of the Lyapunov function becomes

$$\begin{aligned}\dot{\mathrm{V}} &= v^T V^c + \alpha\hat{v}^T\mathcal{L}\hat{x} + \hat{v}^T\Lambda^{-1}(-\alpha\widehat{\mathcal{L}}\bar{x} - \Lambda^2 V^c - \beta v) \\ &= \alpha\hat{v}^T\mathcal{L}\hat{x} + \hat{v}^T(-\alpha\mathcal{L}\hat{x} - \beta\hat{v}) \\ &= -\beta\hat{v}^T\hat{v} \leq 0.\end{aligned} \tag{15}$$

This shows $\dot{\mathrm{V}}$ is negative semi-definite. Let us rewrite (13) as

$$\mathrm{V} = \sum_{i=1}^{n}\sum_{j\in\mathcal{N}_i}\frac{1}{2}V_{ij}^c + \frac{\alpha}{2}\hat{x}^T\mathcal{L}\hat{x} + \frac{1}{2}\hat{v}^T\hat{v}. \tag{16}$$

Here, as $\mathcal{L}$ is positive semi-definite and $V_{ij}^c \geq 0$, it is obvious that V is positive semi-definite. Besides, if V is initially finite, since $\dot{\mathrm{V}}$ is negative semi-definite from (15), V is finite all the time, i.e.,

$$\mathrm{V}(t) \leq \mathrm{V}(0) \ll \infty, \quad \forall t \geq 0.$$

From (16), this implies

$$\sum_{i=1}^{n}\sum_{j\in\mathcal{N}_i}\frac{1}{2}V_{ij}^c \leq \mathrm{V}(t) \leq \mathrm{V}(0) \ll \infty, \quad \forall t \geq 0. \tag{17}$$

There are only two singularities for V_{ij}^c. One is $\|x_{ij}\| = 0$ and the other is $\lambda_{2,i} = \epsilon$. Accordingly, (17) means the control law (7) allows neither of the singularities. Hence, the proposed control law achieves both collision avoidance and connectivity preservation. More specifically, since V is initially finite by the condition, $\|x_{ij}(0)\| > 0,\ \forall i, j \in \mathcal{V}$. Besides, the following equation holds from (17):

$$\|x_{ij}(t)\| > 0, \quad \forall i, j \in \mathcal{V},\ i \neq j,\ \forall t \geq 0 \tag{18}$$

ensuring the agents never collide with each other. At the same time, because $\lambda_{2,i}(0) > \epsilon$, one can easily notice that

$$\lambda_{2,i}(t) > \epsilon \quad \forall i \in \mathcal{V},\ \forall t \geq 0. \tag{19}$$

From (19), the MAS maintains the connectivity all the time. Let $\Omega = \{(\bar{x}(t), v(t)) \mid \mathrm{V}(t) \leq \mathrm{V}(0),\ \forall t \geq 0\}$. From the LaSalle's invariance principle, every solution starting in Ω approaches to the largest invariant set $\mathcal{M} = \{(\bar{x}(t), v(t)) \in \Omega \mid \dot{\mathrm{V}}(t) = 0\}$ as $t \to \infty$ [15]. In (15), $\dot{\mathrm{V}} = 0$ iff $\hat{v}_i = 0$, $\forall i \in \mathcal{V}$ which yields $v_1 = v_2 = \cdots = v_n = 0$, i.e., all agents achieve the stationary velocity consensus. Furthermore, since $u_i = \dot{v}_i = 0$ when the system converges, the following equation can be derived from (7):

$$u_i = \dot{v}_i = -\sum_{j\in\mathcal{N}_i}\left[\alpha(\bar{x}_i - \frac{\omega_i}{\omega_j}\bar{x}_j) + \omega_i^2\nabla_{x_i}V_{ij}^c\right] = 0. \tag{20}$$

If $\|x_{ij}\| \notin (R', R)$ and $\|x_{ij}\| \notin (0, s)$, $\forall (i, j) \in \mathcal{E}$ when the system converges, (20) can be rewritten as

$$u_i = -\sum_{j\in\mathcal{N}_i}\alpha(\bar{x}_i - \frac{\omega_i}{\omega_j}\bar{x}_j) = 0 \tag{21}$$

since V^c is 0_n in that region and accordingly,

$$u = -\alpha\widehat{\mathcal{L}}\bar{x} = -\alpha\Lambda\mathcal{L}\hat{x} = 0_n,$$

where $\bar{x} = [\bar{x}_1, \bar{x}_2, \ldots, \bar{x}_n]^T$. Then, from the fact that the null space of $\mathcal{L}$ is $span\{1_n\}$ if the network is connected, $u = 0_n$ iff $\hat{x} = span\{1_n\}$, i.e., the MAS reaches the consensus [19]. Accordingly, the system with dynamics (1) and control input(7) converges to the local minimum of V, which is the exact desired formation ($\delta = 0$) [7], [22]. Nonetheless, because of complex dynamic interaction between the agents, this condition is hard to be satisfied all the time. Then, due to extra inputs from (8), the formations could be slightly dispersed yielding the quasi-formation. ■

In comparison with (21), (20) has the additional potential function term, $\omega_i^2\nabla_{x_i}V_{ij}^c$. Since the only region $\nabla_{x_i}V_{ij}^c = 0$ is $[s, R')$ for neighboring agents i and j, (9) should be satisfied to minimize the effect of $\omega_i^2\nabla_{x_i}V_{ij}^c$.

From (7), in the static network,

$$u(t) = -\alpha\widehat{\mathcal{L}}\bar{x}(t) - \Lambda^2 V^c(t) - \beta v(t).$$

To extend the result to the dynamic network, let $\mathcal{G}(t)$ be the graph of the network at time t and the corresponding Laplacian matrix as $\mathcal{L}_{\mathcal{G}(t)}$. Then, (7) can be rewritten as follow:

$$u(t) = -\alpha\widehat{\mathcal{L}}_{\mathcal{G}(t)}\bar{x}(t) - \Lambda^2 V^c(t) - \beta v(t) \tag{22}$$

In (22), the control input is a piecewise continuous function which may jump when the graph at time t, $\mathcal{G}(t)$, switches. Such system with the time-varying network can be regarded as the switching system [23]. For the stability analysis of the switching system, the concept of dwell time can be used. It is well known that if each subsystem is asymptotically stable, the stability of the switching system can be guaranteed using the Minimum Dwell Time (MDT) or the Average Dwell Time (ADT) [12], [23], [31]. Since the zeno behavior or the chattering is out of our scope, we simply assume that the dwell time between two distinct network graphs is sufficiently large in this paper. More specifically, define $t_k,\ k = 1,\ 2,\ \cdots$ as the time instant when the network changes. At t_k, the graph varies its configuration by adding or deleting edges. Furthermore, assume the network is fixed during the time interval $[t_k,\ t_{k+1})$ where $t_{k+1} > t_k$. In this paper, we define the dwell time, $\tau(t)$, as follow:

$$\tau(t_k) = t_{k+1} - t_k, \quad \forall k \in \mathbb{N}$$

Assumption 1: There exist MDT, τ_d, which satisfies $t_{k+1} - t_k = \tau(t_k) \geq \tau_d > 0, \forall k \in \mathbb{N}$ and τ_d is sufficiently large to guarantee the stability of the given switching system.

Furthermore, define $\mathcal{G}_c$ as a set of all possible connected graphs. Then, as shown in Theorem 1, if the system starts from the graph in $\mathcal{G}_c$, it would not have graph other than element of $\mathcal{G}_c$, i.e., if $\mathcal{G}(0) \in \mathcal{G}_c$, then $\mathcal{G}(t) \in \mathcal{G}_c,\ \forall t \geq 0$.

Corollary 1.1: If Theorem 1 and Assumption 1 hold, the corresponding MAS is stable in the dynamic network.

Proof: Since $\tau_d \leq \tau(t_k)$ is sufficiently large and every network starts from $\mathcal{G}(0) \in \mathcal{G}_c$ is asymptotically stable, the proposed switching system is also asymptotically stable. ■

Algorithm 1 Decentralized Multi-Subgroup Formation Algorithm

Assume the conditions in Theorem 1 are satisfied $\forall i \in \mathcal{V}$:
initialize $z_1^i,\ z_2^i$, and $\dot{v}_i,\ \forall i \in \mathcal{V}$ for connectivity estimation
  while operation time $t > 0$ **do**
    for all agent $i \in \mathcal{V}$ **do**
      while $\lambda_{2,i}$ is not converged **do**
        $z_1^i, z_2^i \leftarrow$ PI consensus estiamtors from (10)
        $\dot{v}_i \leftarrow$ eigenvector estimation update using (11)
        $\lambda_{2,i} \leftarrow$ estimate the connectivity using (12)
      end while
      for all $j \in \mathcal{N}_i$ **do**
        $V_{ij}^c \leftarrow$ calculate the potential function using (8)
      end for
      $u_i \leftarrow$ calculate the control input using (7)
    end for
    update velocity and poistion using (1)
  end while

We want to emphasize again that the proposed control law (7) does not require the spanning tree within each subgroups; as long as the entire network is initially connected with $\lambda_2 > \epsilon$. This is distinct advantage of the multi-consensus approach in comparison with existing multi-formation algorithms. Although the agents may not receive the information of other agents in the same subgroup, each subgroup can accomplish the separated formation according to ω. For instance, in the original multi-consensus algorithm [11], the convergence point is exactly proportional to the magnitude of ω.

Algorithm 1 explains the procedure of multi-subgroup formation control. Users can freely adjust formation configuration (ρ_i) and subgroup allocation (ω_i) even when the algorithm is running, as long as the conditions in Theorem 1 hold.

IV. NUMERICAL SIMULATION

A. MULTI-SUBGROUP FORMATION SIMULATION

To verify the proposed algorithm, 20 agents are used to generate three separate formations. All agents are deployed with random initial positions and velocities within a certain bound. Among them, 6, 6, and 8 agents are tasked to gather with the intelligence degree (ω) of 1, 1.5, and 2, respectively.

The entire MAS is set to be initially connected, but each subgroup is not connected at the beginning. The desired formation configuration is described in Fig. 6. Other relevant parameters can be found in Table 1. The simulation is run on the 2-D environment.

In Fig. 7(a), the initial positions are displayed showing that the entire network is initially connected. In the figure, the black line means the connection between agents. Six red agents are allocated with $\omega = 1$, whereas 6 green agents and 8 blue agents are allocated with $\omega = 1.5$ and $\omega = 2$, respectively. All subgroups do not have the spanning tree at

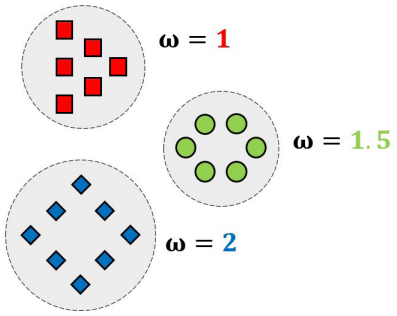

FIGURE 6. Desired formation for the simulation.

TABLE 1. Parameters for numerical simulations.

Parameter	Value
Communication range, R	55 [m]
Formation-limit range, R'	50 [m]
Repulsive range, s	5 [m]
Potential function gain, (k_1, k_2, k_3)	(10, 5, 0.01)
Control constant, (α, β)	(1.5, 1.5)
Intelligence degree, ω	(1, 1.5, 2)
Decay rate, τ	0.5
Connectivity lower bound, ϵ	0.2

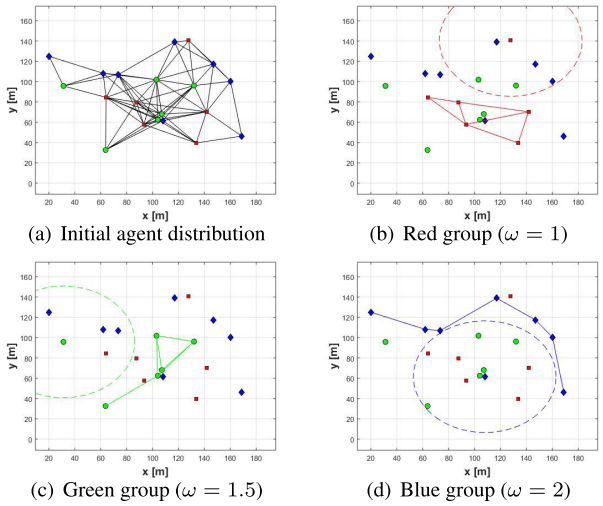

FIGURE 7. Initial network topology for subgroups.

the beginning, i.e., disconnected, shown in Fig. 7(b)-(d). The dashed circles represent the communication range of agents.

Fig. 8(a)-(d) are the time histories. The relative distance between agents is displayed in Fig. 8(e). This result proves the collision avoidance capability of the proposed control law. Fig. 8(f) shows the connectivity of the network during the simulation. One can easily notice that λ_2 never goes lower than ϵ.

B. COMPARATIVE SIMULATION

In this subsection, a comparative simulation without the potential function (8) is provided. From the result, the effectiveness of the proposed algorithm can be emphasized. All conditions are the same with the previous subsection, but

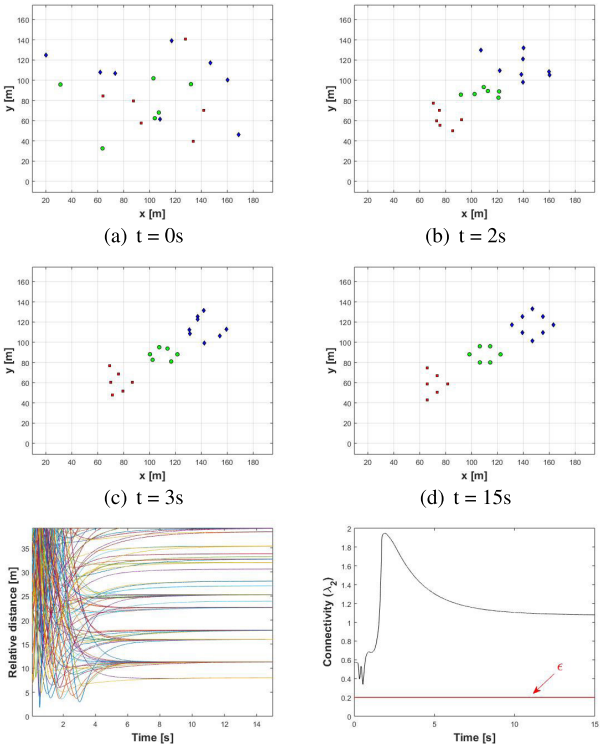

FIGURE 8. Simulation results of the multi-subgroup formation control.

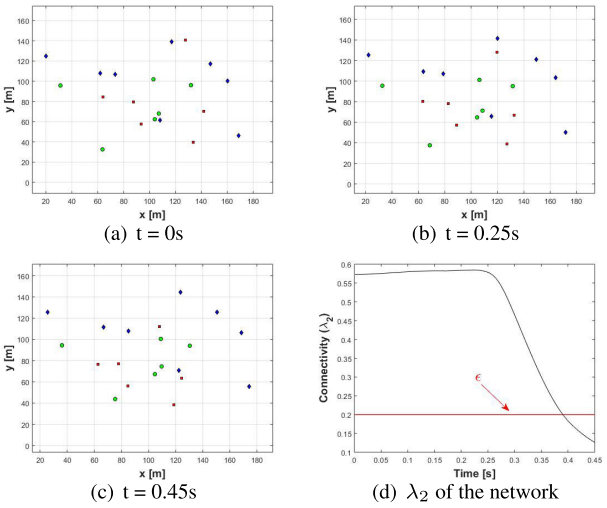

FIGURE 9. Simulation result without the potential function.

the control law does not include the potential function. As a result, the control input for the agent i becomes

$$u_i = -\alpha \sum_{j \in \mathcal{N}_i} (\overline{x_i} - \frac{\omega_i}{\omega_j} \overline{x_j}) - \beta v_i.$$

Fig. 9 shows the results of the simulation where Fig. 9(a)-(c) are the time histories of the agents. In Fig. 9(d), the λ_2 decreases rapidly below ϵ, and the MAS eventually fails to establish the desired formations as well as preserve the network connectivity.

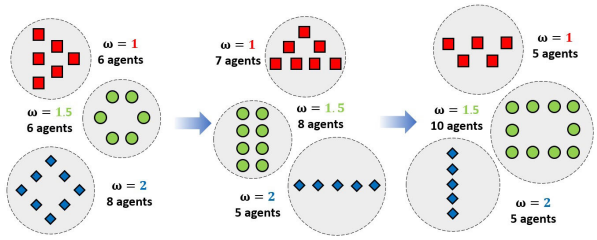

FIGURE 10. Scenario of time-varying formations.

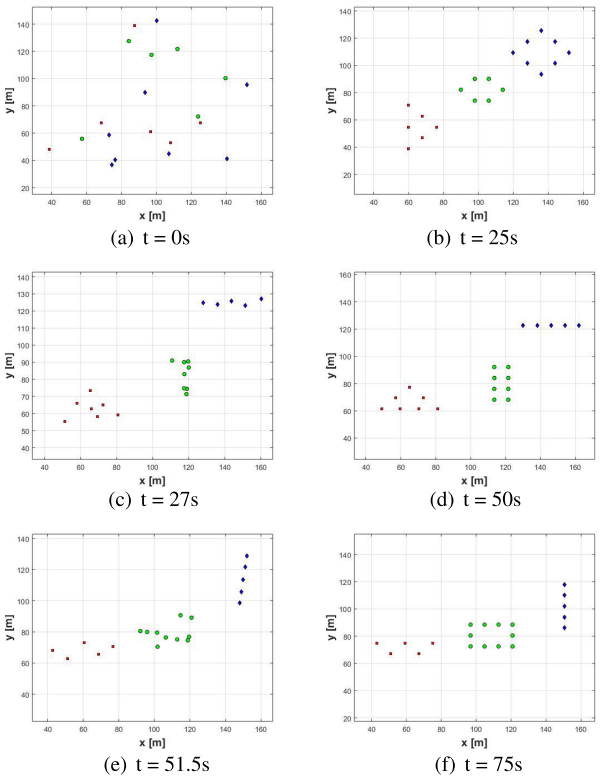

(a) t = 0s (b) t = 25s (c) t = 27s (d) t = 50s (e) t = 51.5s (f) t = 75s

FIGURE 11. Time histories during the time-varying formation scenario.

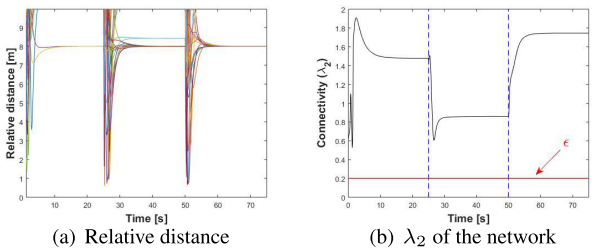

(a) Relative distance (b) λ_2 of the network

FIGURE 12. λ_2 and relative distance histories during the time-varying formation scenario.

C. DYNAMIC FORMATIONS

In this subsection, the simulation results for time-varying formations are provided to show the flexibility of the proposed algorithm. In the simulation, not only the desired formations but also the number of agents assigned to each formation is changed. The detailed environment for the formations is illustrated in Fig. 10. The parameters used for the simulation are identical with the previous one as in Table 1.

Fig. 11 shows the time histories of the position during the simulation. Despite the ordered configurations are dynamically changing, the MAS succeeds to establish the desired formations. Fig. 12(a) and (b) are the relative distance and λ_2 of the MAS, respectively. In Fig. 12(b), the blue dashed line means the moment when the ordered configuration is changed. The proposed algorithm never experiences collision and disconnection even with the dynamically varying formations.

V. CONCLUSION AND FUTURE WORK

This paper has proposed the algorithm that can divide mobile agents into multiple formations without collision and network connectivity lost. By combining modified Multi-Consensus approach with the potential function, the MAS can achieve multi-formation mission without needing initial joint connection between same subgroup members. As future work, the dynamic consensus will be addressed; The proposed algorithm only presents the stationary consensus, i.e., every formations will stop after they converge. Due to this limitation, the algorithm is hard to be applied to non-holonomic vehicles. Another topic is the optimization for subgroup allocation. The optimal allocation for the maximum efficiency might be varied depending on the environments and mission requirements. Moreover, allocating the optimal subgroup per each agent in a decentralized system is challenging. This issue could be solved by the decentralized optimal allocation algorithm.

REFERENCES

[1] F. S. Cattivelli and A. H. Sayed, "Modeling bird flight formations using diffusion adaptation," *IEEE Trans. Signal Process.*, vol. 59, no. 5, pp. 2038–2051, May 2011.

[2] D. F. Chichka, J. L. Speyer, C. Fanti, and C. G. Park, "Peak-seeking control for drag reduction in formation flight," *J. Guid., Control, Dyn.*, vol. 29, no. 5, pp. 1221–1230, Sep. 2006.

[3] H.-L. Choi, L. Brunet, and J. P. How, "Consensus-based decentralized auctions for robust task allocation," *IEEE Trans. Robot.*, vol. 25, no. 4, pp. 912–926, Aug. 2009.

[4] J. Choi, Y. Song, S. Lim, and H. Oh, "Decentralized multiple V-formation control in undirected time-varying network topologies," in *Proc. Workshop Res., Edu. Develop. Unmanned Aerial Syst. (RED UAS)*, Nov. 2019, pp. 278–286.

[5] X. Dong, Q. Li, Q. Zhao, and Z. Ren, "Time-varying group formation analysis and design for general linear multi-agent systems with directed topologies," *Int. J. Robust Nonlinear Control*, vol. 27, no. 9, pp. 1640–1652, 2017.

[6] H. Duan and H. Qiu, "Unmanned aerial vehicle distributed formation rotation control inspired by leader-follower reciprocation of migrant birds," *IEEE Access*, vol. 6, pp. 23431–23443, 2018.

[7] H. Fang, Y. Wei, J. Chen, and B. Xin, "Flocking of second-order multi-agent systems with connectivity preservation based on algebraic connectivity estimation," *IEEE Trans. Cybern.*, vol. 47, no. 4, pp. 1067–1077, Apr. 2017.

[8] R. A. Freeman, P. Yang, and K. M. Lynch, "Stability and convergence properties of dynamic average consensus estimators," in *Proc. 45th IEEE Conf. Decis. Control*, Dec. 2006, pp. 338–343.

[9] X. Ge, Q.-L. Han, and X.-M. Zhang, "Achieving cluster formation of multi-agent systems under aperiodic sampling and communication delays," *IEEE Trans. Ind. Electron.*, vol. 65, no. 4, pp. 3417–3426, Apr. 2018.

[10] G.-S. Han, D.-X. He, Z.-H. Guan, B. Hu, T. Li, and R.-Q. Liao, "Multi-consensus of multi-agent systems with various intelligences using switched impulsive protocols," *Inf. Sci.*, vols. 349–350, pp. 188–198, Jul. 2016.

[11] T. Han, Z.-H. Guan, M. Chi, B. Hu, T. Li, and X.-H. Zhang, "Multi-formation control of nonlinear leader-following multi-agent systems," *ISA Trans.*, vol. 69, pp. 140–147, Jul. 2017.
[12] J. P. Hespanha and A. S. Morse, "Stability of switched systems with average dwell-time," in *Proc. 38th IEEE Conf. Decis. Control*, vol. 3, Dec. 1999, pp. 2655–2660.
[13] Y. Hu, Y. Yao, Q. Ren, and X. Zhou, "3D multi-UAV cooperative velocity-aware motion planning," *Future Gener. Comput. Syst.*, vol. 102, pp. 762–774, Jan. 2020.
[14] Y. Hu, X. Zhou, and Y. Yao, "Decentralized velocity-aware motion planning for multi-agent coordination," in *Proc. IEEE Int. Conf. Service-Oriented Syst. Eng. (SOSE)*, Apr. 2019, pp. 319–324.
[15] H. K. Khalil, *Nonlinear Systems*. Upper Saddle River, NJ, USA: Prentice-Hall, 2002.
[16] E. Kim and D. Choi, "A 3D ad hoc localization system using aerial sensor nodes," *IEEE Sensors J.*, vol. 15, no. 7, pp. 3716–3723, Jul. 2015.
[17] J. Liu, J.-A. Fang, Z. Li, and G. He, "Formation control with multiple leaders via event-triggering transmission strategy," *Int. J. Control, Automat. Syst.*, vol. 17, no. 6, pp. 1494–1506, Jun. 2019.
[18] Y. Mao, L. Dou, H. Fang, J. Chen, and T. Cai, "Distributed flocking of second-order multi-agent systems with global connectivity maintenance," in *Proc. Amer. Control Conf.*, Jun. 2013, pp. 976–981.
[19] M. Mesbahi and M. Egerstedt, *Graph Theoretic Methods in Multiagent Networks*. Princeton, NJ, USA: Princeton Univ. Press, 2010, vol. 33.
[20] H. Oh, S. Kim, H.-s. Shin, and A. Tsourdos, "Coordinated standoff tracking of moving target groups using multiple UAVs," *IEEE Trans. Aerosp. Electron. Syst.*, vol. 51, no. 2, pp. 1501–1514, Apr. 2015.
[21] K.-K. Oh, M.-C. Park, and H.-S. Ahn, "A survey of multi-agent formation control," *Automatica*, vol. 53, pp. 424–440, Mar. 2015.
[22] R. Olfati-Saber, "Flocking for multi-agent dynamic systems: Algorithms and theory," Control Dyn. Syst., California Inst. Technol., Pasadena, CA, USA, Tech. Rep. CIT-CDS 2004-005. [Online]. Available: https://resolver.caltech.edu/CaltechCDSTR:2004.005
[23] H. Pan and X.-H. Nian, "Consensus of second-order multi-agent system under average dwell-time switching topologies," in *Proc. 33rd Chin. Control Conf.*, Jul. 2014, pp. 1716–1721.
[24] M. Park and H. Oh, "Cooperative information-driven source search and estimation for multiple agents," *Inf. Fusion*, vol. 54, pp. 72–84, Feb. 2020.
[25] H.-S. Shin, A. J. Garcia, and S. Alvarez, "Information-driven persistent sensing of a non-cooperative mobile target using UAVs," *J. Intell. Robot. Syst.*, vol. 92, nos. 3–4, pp. 629–643, Dec. 2018.
[26] X. Dong, Q. Li, Q. Zhao, and Z. Ren, "Time-varying group formation analysis and design for second-order multi-agent systems with directed topologies," *Neurocomputing*, vol. 205, pp. 367–374, Sep. 2016.
[27] G. Vásárhelyi, C. Virágh, G. Somorjai, N. Tarcai, T. Szörényi, T. Nepusz, and T. Vicsek, "Outdoor flocking and formation flight with autonomous aerial robots," in *Proc. IEEE/RSJ Int. Conf. Intell. Robots Syst.*, Sep. 2014, pp. 3866–3873.
[28] G. Vásárhelyi, C. Virágh, G. Somorjai, T. Nepusz, A. E. Eiben, and T. Vicsek, "Optimized flocking of autonomous drones in confined environments," *Sci. Robot.*, vol. 3, no. 20, Jul. 2018, Art. no. eaat3536.
[29] H. Wu, H. Li, R. Xiao, and J. Liu, "Modeling and simulation of dynamic ant colony's labor division for task allocation of UAV swarm," *Phys. A, Stat. Mech. Appl.*, vol. 491, pp. 127–141, Feb. 2018.
[30] P. Yang, R. A. Freeman, G. J. Gordon, K. M. Lynch, S. S. Srinivasa, and R. Sukthankar, "Decentralized estimation and control of graph connectivity for mobile sensor networks," *Automatica*, vol. 46, no. 2, pp. 390–396, Feb. 2010.
[31] G. Zhai, B. Hu, K. Yasuda, and A. N. Michel, "Piecewise Lyapunov functions for switched systems with average dwell time," *Asian J. Control*, vol. 2, no. 3, pp. 192–197, 2000.

JOONWON CHOI was born in Seoul, South Korea, in 1994. He received the B.S. degree in mechanical and aerospace engineering from the Ulsan National Institute of Science and Technology (UNIST), Ulsan, in 2019. Since 2019, he has been a Researcher with the Autonomous Systems Laboratory, UNIST. His research interests include multiagent system and application, formation control, autonomous landing, and high-level control algorithm for autonomous systems.

YEONGHO SONG received the B.S. degree in mechanical and aerospace engineering from the Ulsan National Institute of Science and Technology (UNIST), Ulsan, in 2017, where he is currently pursuing the Ph.D. degree. His research interests include optimization-based control with applications, multiagent systems, and flocking control for unmanned aerial vehicles.

SEUNGHAN LIM was born in Seoul, South Korea, in 1981. He received the B.S. degree in aerospace engineering from Inha University, Incheon, South Korea, in 2007, and the M.S. and Ph.D. degrees in aerospace engineering from the Korea Advanced Institute of Science and Technology (KAIST), Daejeon, South Korea, in 2009 and 2013, respectively. In 2013, he was a Senior Researcher with the Agency for Defense Development (ADD), Daejeon. His research interests include guidance and control law for single unmanned aircraft, swarming behavior control for multiple unmanned aircraft, and decision theory for cooperation and collaboration among human and multiple unmanned aircraft.

CHEOLHYEON KWON (Member, IEEE) received the B.S. degree in mechanical and aerospace engineering from Seoul National University, Seoul, South Korea, in 2010, and the M.S. and Ph.D. degrees from the School of Aeronautics and Astronautics, Purdue University, West Lafayette, IN, USA, in 2013 and 2017, respectively. He is currently an Assistant Professor with the School of Mechanical, Aerospace and Nuclear Engineering, Ulsan National Institute of Science and Technology (UNIST), Ulsan, South Korea. His research interests include control and estimation for dynamical cyber-physical systems (CPS), along with networked autonomous vehicles, air traffic control systems, sensors and communication networks, and cybersecure and high assurance CPS design, inspired by control and estimation theory perspective, with applications to aerospace systems, such as unmanned aircraft systems (UAS).

HYONDONG OH (Senior Member, IEEE) received the B.Sc. and M.Sc. degrees in aerospace engineering from the Korea Advanced Institute of Science and Technology (KAIST), South Korea, in 2004 and 2010, respectively, and the Ph.D. degree in autonomous surveillance and target tracking guidance (multiple UAVs) from Cranfield University, U.K., in 2013. He was a Lecturer in autonomous unmanned vehicles with Loughborough University, U.K., from 2014 to 2016. He is currently an Associate Professor with the School of Mechanical, Aerospace and Nuclear Engineering, Ulsan National Institute of Science and Technology (UNIST), South Korea. His research interests include autonomy and decision making, cooperative control and path planning, nonlinear guidance and control, estimation and sensor/information fusion for unmanned systems.